Modelling and Control of Electromagnetic Vibratory Actuator Applied in Vibratory Conveying Drives

Željko V. Despotović, Aleksandar I.Ribić
Department of Robotics
Mihajlo Pupin Institute, University of Belgrade
Belgrade, Serbia
Volgina 15, Belgrade, zeljko.despotovic@pupin.rs

Vladimir Šinik
Technical Faculty "Mihajlo Pupin"
University of Novi Sad
Zrenjanin, Serbia

Abstract—**Modelling and amplitude/frequency control of one typical electromagnetic vibratory actuator are presented. Electromagnetic vibrating actuators are widely used as drives of vibratory conveyors and vibratory feeders. A resonant type vibratory drive is discussed. By suitable power converters and related PWM control one can achieve adjusting vibratory excitation force of vibratory actuator, i.e. vibratory conveying of particulate materials on conveyor load carrying element. Simulation model of the vibratory actuator has been generated by using program MATLAB. This model can be used as integral part of the simulation circuit (power converter and control circuit). The corresponding simulation and experimental results and their comparisons are presented. The experimental results are recorded by the practically implemented IGBT power converter and control system based on a PC104 module.**

Key words- Vibration control;actuator; power converter; IGBT; vibratory conveying; modelling; MATLAB;

I. INTRODUCTION

The vibratory conveyors and feeders having electromagnetic vibratory drives provide easy flow of particulate materials. Their application is widely used in various manufacturing industries (food, pharmaceutical, cement, etc). These vibrating machines are very popular because of their high efficiency and easy maintenance. This applies in particular to resonant vibratory conveying drives. However, their performance is highly sensitive to different kinds of disturbances. For example, as the conveyor (feeder) vibrations occur at its resonance frequency, vibration amplitude is highly dependent on damping factor. On the other hand, damping factor depends on the mass of material on the feeder through, type of material, and vibration amplitude [1]. These disturbances can reduce drastically (up to 10 times) the vibration amplitude, thus reducing the performance of the whole vibratory conveying drive. A key element that compensates these influences is the electromagnetic vibratory actuator (EVA) which is based on electromagnetic induction principle [2]. Also, vibration control of EVA is a very significant factor in resolving the aforementioned problem. The application of EVA in combination with power converter provides control flexibility. By providing operation of the vibratory conveying system in the region of the mechanical resonance, it behaves as the controllable mechanical oscillator [2-3]. In the present paper by combining IGBT power converter for driving EVA [4-6] with a feedback PI controller and state observer, a fast set point and disturbance rejection responses of the vibratory conveying drive are obtained. A high performance feedback controller is implemented on industrial PC platform and applied to the experimental conveyor. The simulations and experimental results confirm effectiveness of the proposed controller.

II. DESCRIPTION OF VIBRATORY CONVEYING SYSTEM

A typical arrangement of vibratory conveying system with EVA is shown in Fig.1. Its main components are the *load carry element (LCE)*-1, electromagnetic vibratory actuator (EVA) as source of excitation force F , and *flexible elements*- 2. Flexible elements (leaf springs) are made of a fiberglass composite material. These elements are rigidly connected to the *base*-3, which is resting on dumping *rubber mounts*-4 set on the foundation. EVA consists of *magnetic core*-5 covered by continuous *windings coil*-6. Electromagnetic driving force F acts on *armature*-**7** rigidly attached to the LCE. This element carries the *vibratory trough*-8 along with particulate conveying material. The vibratory displacement is measured by a no-contact *inductive sensor*-9.

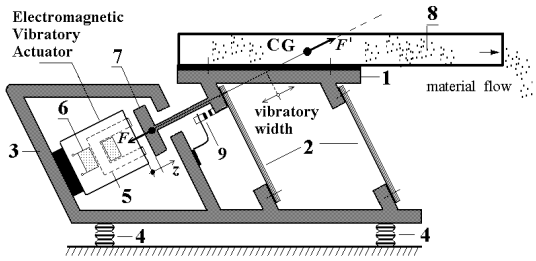

Figure1. Typical construction of a vibratory conveying system having electromagnetic vibratory actuator.

The previously described electromechanical system represents starting point for the creation of a mathematical model of EVA which drives LCE including particulate material. Since the mass of conveying material is variable, EVA will operate in regimes involving variable load, so it is necessary to make a correct stabilization of its operation [7-9].

III. MODELLING OF ELECTROMAGNETIC VIBRATORY ACTUATOR

Fig.2 shows basic overview of the modelling vibrating system described in the previous section. The equivalent electromechanical model is shown in Fig.2 (a). This model consists of the electromagnetic and mechanical parts. The electromagnetic model of EVA is shown in Fig. 2(b). An

This investigation has been carried out with the financial support of the Serbian Ministry of Education, Science and Technological Development - project No: TR33022.

electromagnet is connected to an AC source and the reactive section is mounted on an elastic system of composite springs. During each half period when the maximum value of the current is reached, the armature is attracted, and at a small current value it is repelled as a result of the elastic forces in the springs. Therefore, vibratory frequency is double the frequency of the power supply. This reactive vibratory actuator can also operate on interrupted, pulsating (DC) current. Their frequency in this case depends on the pulse frequency of the DC.

Mechanical force, created by electromechanical conversion in the EVA, is transmitted from LCE to the particulate material. It is assumed that the mass of load M is much greater than the mass of the movable armature. Let us suppose that the composite springs are identically constructed, with stiffness k .The nonlinearity of spring elements is neglected. Total equivalent damping coefficient of the system is β . Movement of the inductor is restricted to the z -direction. At initial moment $t = 0$ gravitational force is compensated by the spring forces. Detailed model of EVA, derived in [6], can be written as:

$$L(z)\cdot\frac{di}{dt}+\left(\frac{\partial L(z)}{\partial z}\cdot\frac{dz}{dt}+R\right)\cdot i = u\,, \qquad (1)$$

$$F=\frac{1}{2}\frac{\partial L(z)}{\partial z}\cdot i^2\,, \qquad (2)$$

where R_c and $L(z)$ denote coil electrical resistance and inductivity, and z , i , and u denote armature position in relation to fixed conveyor base, coil current, and coil voltage respectively. Equivalent electrical scheme of EVA is shown in Fig.2 (c). Relation (2) gives the mechanical force F produced by the EVA. The expression for the inductance $L(z)$ is mathematically derived in references [2-3], [6]. Thus, inductance $L(z)$ can be presented by expression:

$$L(z)=L_0\cdot\frac{z_0}{z}\,,\ z_{\max}z\geq d\,. \qquad (3)$$

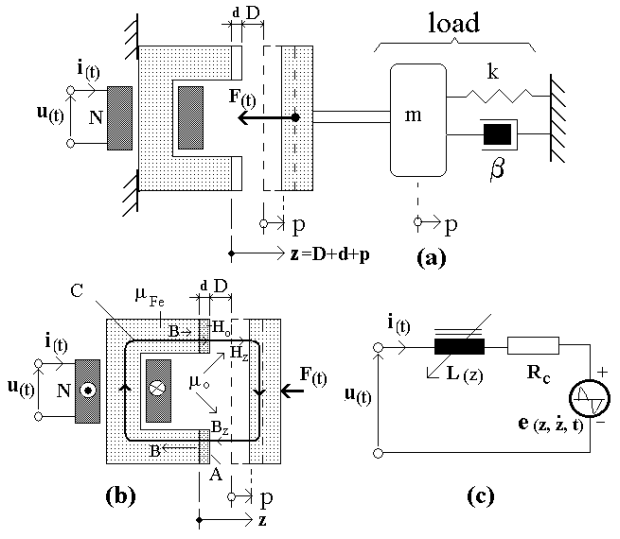

Figure 2. Electromechanical model of vibratory conveying system; (a) electromechanical part, (b) electromagnet of actuator, (c) equivalent electrical scheme.

Inductance of the EVA in equilibrium position (when $z = z_0 = D + d$, i.e. $p = 0$) L_0 is given by relation:

$$L_0=\frac{2\mu_0 N^2 A}{D+d}\,. \qquad (4)$$

It is supposed that the ferromagnetic core of EVA has a very high permeability μ_{Fe} (reluctance of the magnetic core path can be ignored) compared to μ_0 of the air gap and bronze disk. Consequently, all the energy of the magnetic field is stored in the air gap and bronze. The area of cross section of the air gap is A . The air gap length in the state of static equilibrium is D . The bronze disk of thickness d does not permit inductor to form a complete magnetic circuit made of iron; in other words, it inhibits *"gluing"* of armature and inductor, which is undesirable. In real cases is $d << z_0$.

If the short excitation current pulse for EVA is synchronized with the instant when the armature is passing through the equilibrium position, i.e. when $z = z_0$, inductance $L(z)$ can be represented, with sufficient accuracy, as $L(z) \approx L_0$. Now, equation (1) in the vicinity of the operating point can be represented as [5], [10]:

$$L_0\cdot\frac{di}{dt}+R_c'\cdot i = u\,. \qquad (5)$$

Parameter R' represents the equivalent resistance which is dependent on the speed of displacing of the LCE and gradient of the coil inductance at the operating point, given by relation:

$$R_c'=R_c+\frac{dp}{dt}\cdot\left.\frac{\partial L}{\partial p}\right|_{p=p_0}\,. \qquad (6)$$

Taking into account that the excitation current pulses of EVA are short (of the order of several milliseconds), it can be assumed that the equivalent time constant L_0 / R_c' is much longer than their duration. On the basis of this, it can be concluded that $R_c' \cdot i << u$. Therefore, member $R_c' \cdot i$ in equation (5) can be neglected [10]. Finally, the approximation of equation (5) is given by:

$$\frac{di}{dt}=\frac{u}{L_0}\,. \qquad (7)$$

As already mentioned, pulse excitation is, from the energy point of view, the most suitable method of excitation of electromagnetic resonant conveyors [11-14] . Owing to the predominantly inductive nature of EVA coil, indicated by equation (7), it is very simple, by applying a suitable control, to generate current pulses in this coil which are of the form of triangular half-waves [4-5], [10].

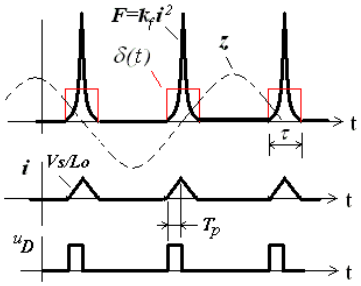

Figure3. Characteristics waveforms for calculating strength of current pulse.

As pulse width T_p in practical applications is very small against the cycling period, its contribution can be approximated by Dirac pulse $\delta(t)$ of the same strength. According to (2), (7), and Fig. 3, strength of the current pulse Q_i can be calculated as follows:

$$Q_i = 2\int_0^{T_p} i^2 dt = \frac{2}{3}\frac{V_S^2}{L_0^2}\cdot T_p^3 . \quad (8)$$

IV. Modelling of Mechanical Load

Detailed dynamic model of the mechanical load of EVA is given in [2-3], [11], [13]. Essential dynamics can be approximated by only one dominant oscillating mode:

$$\ddot{z} + 2\varsigma\cdot\omega_0\cdot\dot{z} + \omega_0^2\cdot(z - z_0) = K_p\cdot\omega_0^2\cdot F , \quad (9)$$

where ω_0 (rad/s), ς, and K_p, denote resonant frequency, damping factor, and static gain of mechanical part of the vibratory system, respectively. However, from the viewpoint of the design and tuning of the control system, we have to analyze simplified model (9) in the presence of the material in the trough. There are two cases important for our analysis [10], [15]:

- When the amplitude is relatively small, material is moving together with trough (there is no transport). In this case material is acting as additional mass.
- At higher amplitudes, transported material is in fluidized state, reacting with a trough as additional damping force.

As will be shown by experimental results, it is assumed that the value of parameter ς is higher (estimated 0.1) and at small amplitudes ς is lower (estimated 0.01), as for empty trough. From the above analysis it follows that the resonant peak, which is inversely proportional to ς, changes by a factor about 10. Since the damping ratio is small, further simplification is adopted by setting $\varsigma = 0$ in (9). Finally, as ω_0 is practically independent of the trough content, model of the mechanical part can be expressed in the following state space form:

$$\dot{x} = \begin{bmatrix}\dot{x}_1\\ \dot{x}_2\end{bmatrix} = \omega_0\cdot\begin{bmatrix}0 & 1\\ -1 & 0\end{bmatrix}\cdot\begin{bmatrix}x_1\\ x_2\end{bmatrix} + K_{p1}\omega_0\cdot\begin{bmatrix}0\\ 1\end{bmatrix}\cdot i^2 , \quad (10)$$

$$x_1 = z - z_0 , \quad (11)$$

$$K_{p1} = \frac{K_p}{2}\cdot\left.\frac{\partial L(z)}{\partial z}\right|_{z=z_0} . \quad (12)$$

Vibration amplitude Z_m is expressed as function of the state x:

$$Z_m = \sqrt{x_1^2 + x_2^2} \quad (13)$$

Now, it is interesting to analyze the response of the previously described model excited by Dirac delta pulse of i^2. From (10) and (13), it is obtained:

$$Z_{m+} = \sqrt{Z_{m-}^2 + 2K_{p1}\omega_0 Q_i x_{2-} + (K_{p1}\omega_0 Q_i)^2} , \quad (14)$$

where - and + signs in indexes indicate values immediately before and after pulse, respectively, and Q is pulse strength. From (14) it follows that the highest increase or decrease of the amplitude is obtained when x_2 is in its maximum or in its minimum, respectively. In both cases:

$$x_1 = 0 , \quad (15)$$

$$x_2 = \pm Z_{m-} . \quad (16)$$

Thus, from (14) – (16) one obtains:

$$Z_{m+} = Z_{m-} \pm K_{p1}\omega_0 Q_i , \quad (17)$$

where ± sign corresponds: + for increasing and – for decreasing of the amplitude.

V. Control System of EVA

The principal structure of the EVA control system is presented in Fig. 4. This control structure consists of the state observer, pulse triggering circuit of IGBT power converter and PI controller.

According to the presented model of the mechanical part, (10)-(12), *Luenberger* observer, described in [16-17], is chosen. The observer model in this specific case is given as:

$$\dot{\hat{x}} = \omega_0\cdot\left\{\begin{bmatrix}-k_1 & 1\\ -1-k_2 & 0\end{bmatrix}\cdot\hat{x} + K_{p1}\cdot\begin{bmatrix}0\\ 1\end{bmatrix}\cdot i^2 + \begin{bmatrix}k_1\\ k_2\end{bmatrix}\cdot(z - z_0)\right\} . \quad (18)$$

Parameters k_1 and k_2 are obtained by defining time constants T_1 and T_2 of the observer as $T_1 = T_2 = \pi/(10\omega_0)$. Thus, $k_1 = 6.3694$ and $k_2 = 9.1424$. Coil current i can be measured or estimated by using signal of u_D and equation (4). Parameter z_0 can also be estimated on line. Its estimation is defined by relation:

$$T_0\dot{\hat{z}}_0 = z - \hat{z}_0 - x_1 , \quad (19)$$

where T_0 is filter time constant. As z_0 changes relatively slowly, T_0 can be comfortably large. It is suggested here to use $T_0 = 10\pi/\omega_0$. Finally, the amplitude is estimated by using $a = \sqrt{\hat{x}_1^2 + \hat{x}_2^2}$. As demonstrated experimentally, this enables fast disturbance rejection. The relationship between time duration τ of EVA current and amplitude increase/decrease is highly nonlinear. By combining equations (8) and (17) one obtains value of pulse width T_p (approximately equal to $\tau/2$):

$$T_p = \sqrt[3]{\frac{3L_0^2}{2V_S^2 K_{p1}\omega_0}|\Delta a|} , \quad (20)$$

where Δa is desired increment ($\Delta a > 0$), or decrement ($\Delta a < 0$) of amplitude, obtained from the controller shown in Fig. 4. In this way, (20) defines pulse width – amplitude linearization. Now, we can define triggering conditions for amplitude increasing:

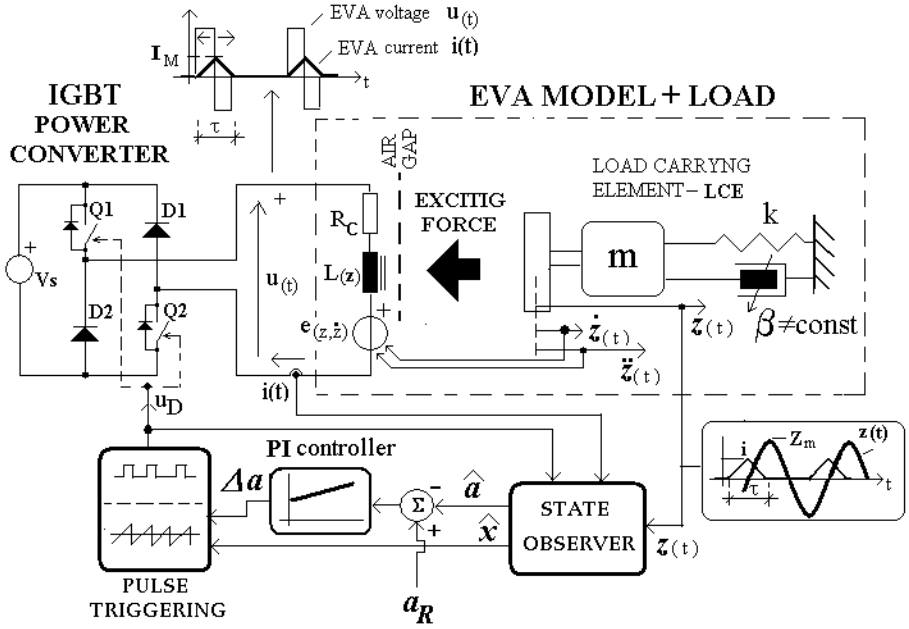

Figure 4. Control structure of EVA.

$$\cos(\omega_0 T_p)\hat{x}_1 + \sin(\omega_0 T_p)\hat{x}_2 \geq 0,\ \hat{x}_1 < 0 \qquad (21)$$

or decreasing:

$$\cos(\omega_0 T_p)\hat{x}_1 + \sin(\omega_0 T_p)\hat{x}_2 \leq 0,\ \hat{x}_1 > 0\,, \qquad (22)$$

providing that at the center of current pulse (end of PWM control u_D pulse after time T_p) condition (11) is satisfied. The simplest control law is the proportional one:

$$\Delta a = K_C(a_R - \hat{a})\,, \qquad (23)$$

where K_C, a_R, and $\hat{a}$ denote controller gain, reference amplitude, and observed amplitude respectively. The value of Δa and the corresponding T_p are calculated in real time until pulse is started. During the pulse, T_p is unchanged. The upper limit for controller gain is $K_C = 1$, meaning that after the pulse, control error has to be zero. In practice, due to the modeling errors and adopted approximations in calculations, recommended gain interval is $K_C \leq 0.8$. To have offset-free control, integral action is introduced, so PI control law, given in literature [18=19], is:

$$\Delta a = K_C\left[(a_R - \hat{a}) + \frac{1}{T_I}\int (a_R - \hat{a})dt\right], \qquad (24)$$

where T_I denotes integral time constant of the controller. It is recommended to choose integral constant $T_I = 10\pi/\omega_0$.

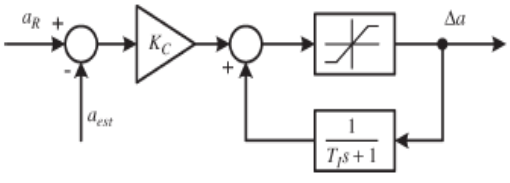

Figure 5. Anti-windup structure of the PI controller.

Anti-windup implementation of PI controller presented in Fig. 5 is used as in [20], with the saturation element providing limit on controller output and, according to (20), with pulse duration T_p.

VI. The Simulation Results

To illustrate the basic operation of the proposed EVA control, the simulations are performed using the simplified models of the electrical and mechanical parts, developed in Sections III and IV. In this analysis real values of parameters of EVA and mechanical load are: force gain $k_f = 50$ ($f = k_f i^2$), $V_S / L_0 = 150$, $K_p = 1$, $\omega_0 = 314$ rad/s ($f_0 = 50Hz$), $\varsigma \in [0.01, 0.1]$. The controller presented in Section 5 is implemented in digital form, with sampling period $T_s = 0.1$ms and 0.025mm conversion resolution. Pulse duration T_p is limited on a maximum value of 4ms.

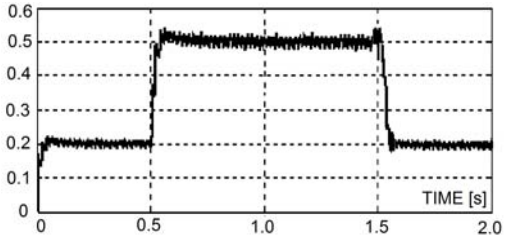

Figure 6. Simulated amplitude response on reference change.

Fig. 6 illustrates behavior of the control loop in the presence of reference changes and disturbance. At $t = 0.5$s reference of amplitude is changed from $a_R = 0.2$mm to $a_R = 0.5$mm, and at $t = 1.5$s back to $a_R = 0.2$mm. Only the estimated amplitude is presented. Integral part of the controller provides that the mean value of amplitude coincides with its reference. Set

point response is fast, with small overshoots in both cases (rising and decreasing).

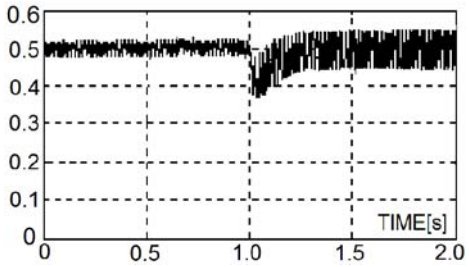

Figure 7. Simulated amplitude response on damping ratio change.

Fig.7 shows amplitude response at a damping ratio change. At reference $a_R = 0.5$mm and moment $t = 1$s there is step change in damping ratio from $\varsigma = 0.01$ to 0.03. Disturbance response has small maximum error and recovery time defined by integral time constant ($T_I = 0.1$s).

VII. The Experimental Results

To demonstrate the performance of the proposed feedback controller, the experimental setup presented in Fig. 1, IGBT power converter, and control system described in Section V are used. The control algorithm is implemented on industrial PC platform with 12bit A/D interface for displacement measurement and Linux + RTAI operating system software. Displacement is measured by inductive distance sensor Ni-10, 0-6mm range, analog output 0-10V, *Turck* production.

To illustrate dynamic characteristics of the EVA load in both cases (empty and full trough), the trough of our experimental conveyor is filled with sugar and the feeder is excited by short current pulse as before. Time responses for the empty and full trough are compared in Fig. 8. In oscilloscopic records of channel CH2, at the beginning, at higher amplitudes, value of parameter ς is higher (estimated 0.1) and at lower amplitudes ς is lower (estimated 0.01), as for empty trough, as shown by channel CH1.

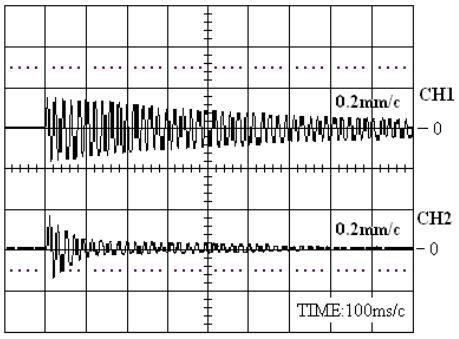

Figure 8. Experimental time responses of the EVA armature displacement: CH1-empty trough, ς=0.01, CH2- fill of sugar, ς=0.1.

Parameters K_{p1} and ω_0 in model (10) – (12) are estimated from the experiment with empty trough. The system is excited by $T_p = 4ms$ pulse on control voltage u_D, $V_S = 300$V, and the response is recorded. Parameter $\omega_0 = 320$rad/s is determined directly from cycle duration. Immediately after the pulse, amplitude Δa reaches its maximum, so K_{p1} is obtained from (18). Parameter L_0 is estimated from the coil current response.

Reference change tests are made for empty and for full trough. Reference is changed in steps from 0.1mm to 1mm and back to 0.1mm. The results are presented in Fig. 9. Both responses are well damped and with small overshoots.

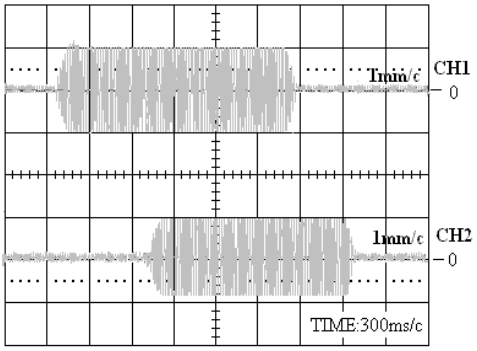

Figure 9. Experimental reference change responses: CH1- empty trough, CH2- full trough.

A 250g particulate material bag dropped onto LCE trough is used to demonstrate disturbance response of the electromagnetic vibratory drive. After about 1 - 1.5s, the bag is removed from the trough. The results are presented in Fig. 10, only for amplitude reference $a_R = 0.5mm$ and for empty trough, when the effect of disturbance is the highest.

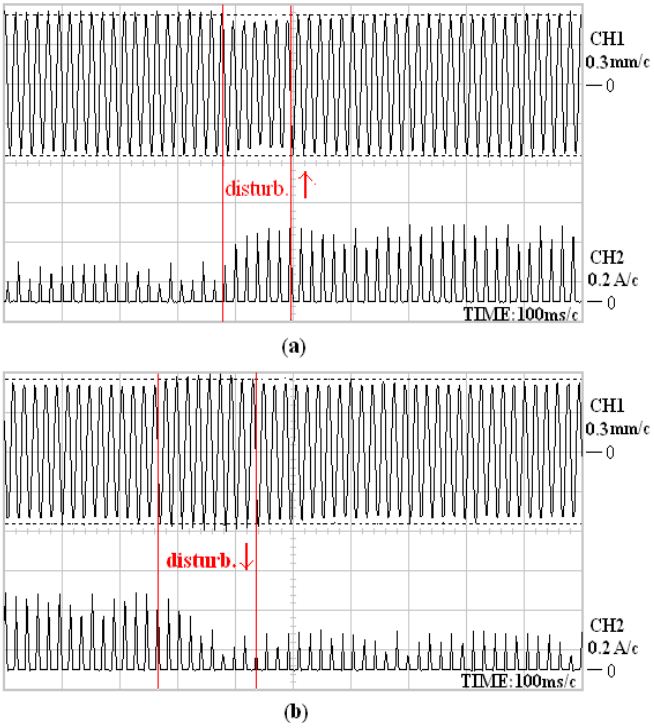

Figure 10. Experimental disturbance change responses for empty trough.

VIII. CONCLUSION

A simple EVA and its load carrying element are analyzed. Despite low price and low maintenance costs, this kind of EVA is often poorly controlled (frequently without feedback), reducing its applicability in precise weighting. A new control structure, based on the state observer and PI controller, proposed in this paper, significantly improves vibratory conveying, thus enabling high performances.

The absence of wearing mechanical part, such as gears, cams belts, bearings, eccentrics or motors, makes EVA one of the most promising devices for application in processing of granular and particulate materials (conveying, dosage weighing, etc.) in various manufacturing industries. They are compact, robust and reliable in operation. Efficient control of the device at its resonant frequency, obtained by small values of EVA coil current, results into small power consumption.

LITERATURE

[1] I.F. Goncharevich, K.V. Frolov, and E.I. Rivin, Theory of vibratory technology, Hemisphere Publishing Corporation, New York, 1990.

[2] T. Doi, K. Yoshida, Y. Tamai, K. Kono, K. Naito, and T. Ono, "Modeling and Feedback Control for Vibratory Feeder of Electromagnetic Type", Journal of Robotics and Mechatronics, vol. 11, no. 5, pp. 563-572, June 1999.

[3] T. Doi, K. Yoshida, Y. Tamai, K. Kono, K. Naito and T. Ono, "Feedback Control for Electromagnetic Vibration Feeder", JSME International Journal, Series C, vol. 44, no. 1, 2001, pp. 44-52.

[4] Z.Despotovic, A.Ribic,"Low Frequency IGBT Converter for Control Exciting Force of Electromagnetic Vibratory Conveyors", PROCEEDINGS of the XV International Symposium of the Power Electronics, N.Sad 28-30.10.2009, Vol.T1-1.8, pp. 1-5.

[5] Ž.V. Despotović , A. I. Ribić, V.Sinik , Power Current Control of a Resonant Vibratory Conveyor Having Electromagnetic Drive, Journal of Power Electronics, Vol.12, No4, July 2012.

[6] Z. Despotovic and Z. Stojiljkovic, " Power Converter Control Circuits for Two-Mass Vibratory Conveying System with Electromagnetic Drive: Simulations and Experimental Results" , IEEE Transaction on Industrial Electronics, vol. 54, Issue I, February 2007, pp. 453-466.

[7] V.I.Babitsky, "Autoresonant Mechatronics Systems", Mechatronics 5 (1995), pp. 483-495.

[8] I.J.Sokolov, V.I.Babitsky, N.A.Halliwell, "Autoresonant Vibro-impact System with Electromagnetic Excitation ", Journal of Sound and Vibration, 308 (2007), pp. 375-391.

[9] P.U.Frei, "An Intelligent Vibratory Conveyor for the Individual Object Transportation in Two Dimensions" Proceedings of the 2002 IEEE/RSJ, Intl. Conference on Intelligent Robots and Systems, EPFL, Lausanne, Switzerland, October 2002, pp.1832-1837.

[10] A.I.Ribic and Z.Despotovic, " High-Performance Feedback Control of Electromagnetic Vibratory Feeder", IEEE Transation on Industrial Electronics, Vol.57, Issue :9, Aug. 2010,pp.3087-3094.

[11] H.G.Cock "Vibratory Feeders" PHILIPS Technical Review, Vol.24, May 1975, pp.84-95.

[12] L.Han and S.K.Tso, "Mechatronic design of a flexible vibratory feeding system", Proceedings of the I MECH-E- Part B Journal of Engineering Manufacture, Vol.217, No.6, June 2003, pp.837-842.

[13] P.Wolfsteiner, F.Pfeiffer, "Dynamics of a vibratory feeder", PROCEEDINGS of DETC '97, ASME Design Engineering Technical onferences, Sacramento, California, DETC97/VIB-3905, Sept.14-17, 1997, pp.1-9.

[14] M.A. Parameswaran and S. Ganapathy, "Vibratory Conveying-Analysis and Design: A Review", Mechanism and Machine Theory, vol. 14, no. 2, pp. 89-97, April 1979.

[15] T.Yanagida, A.J.Matchett and J.M.Coulthard, "Dissipation Energy of Powder Beds Subject to Vibration" , Trans IChemE, vol. 79, part A, September 2001, pp.655-662.

[16] D. G. Luenberger, "Observing the State of a Linear System," IEEE Trans. Military Electronics, vol. 8, pp. 74–80, April 1964.

[17] D. G. Luenberger, "An introduction to observers" IEEE Trans.Automatic Control, vol. 16, No. 6, pp. 566–602, 1971.

[18] K.J. Astrom, T. Hagglund, "The future of PID control", Control Eng. Practice, vol. 9, pp. 1163-1175, 2001.

[19] S.Skogestad "Simple analytic rules for model reduction and PID controller tuning", Journal of Process Contro,l vol. 13, pp291-309, 2003.

[20] C.Edwards, I. Postlethwaite, "Anti-windup and Bump less-transfer Schemes", Automatica , vol. 34, no. 2, pp. 199-210, 1998.